Engineering Conferences International
ECI Digital Archives

The 14th International Conference on Fluidization – From Fundamentals to Products

Refereed Proceedings

2013

Time- Averaged Simulation of the Furnace of a Commercial CFB Boiler

Juho Peltola
VTT Technical Research Centre of Finland, Finland

Sirpa Kallio
VTT Technical Research Centre of Finland, Finland

Hairui Yang
Tsinghua University, China

Xiaolong Qiu
Tsinghua University, China

Jingji Li
Tsinghua University, China

TIME- AVERAGED SIMULATION OF THE FURNACE OF A COMMERCIAL CFB BOILER

Juho Peltola[a]*, Sirpa Kallio[a], Hairui Yang[b], Xiaolong Qiu[b] and Jingji Li[b]

[a]VTT Technical Research Centre of Finland;
Metallimiehenkuja 6, Espoo; P.O.Box 1000; FI-02044 VTT, Finland
[b]Tsinghua University, Department of Thermal Engineering
Haidian District, Beijing, China
*T: +358 20 359 1860; F: +358 20 722 7077; E: juho.peltola@vtt.fi

ABSTRACT
A time-averaged simulation approach is applied to a 135 MWe circulating fluidized bed combustor located in Ruzhou, China, in which also measurements were carried out. The simulation results show a vertical solids distribution typical for a CFB. Gas composition profiles show plausible but not fully correct distributions of oxygen and combustion products inside the furnace.

INTRODUCTION
Dense gas-solid flows are usually computed as time-dependent requiring a small time step and a fine mesh which lead to time-consuming simulations. To reduce computing time, Taivassalo & al. (1) introduced a time-averaged CFD model and in Taivassalo & al. (2), the approach was applied on CFB combustion in Chalmers 12 MW boiler. In addition to hydrodynamics, models for heat transfer and chemistry, including homogeneous and heterogeneous reaction mechanisms, were included in the modeling. The behavior of fuel particles was simulated with a Lagrangian approach.

The time-averaged simulation approach is applied to a 135 MWe circulating fluidized bed combustor located in Ruzhou, China, to examine how the modeling approach behaves in a commercial scale CFB. A measurement campaign was carried out at 120 MWe load. In the paper, results from the simulations are presented and compared with measurement data, including pressure and temperature distributions and gas composition data.

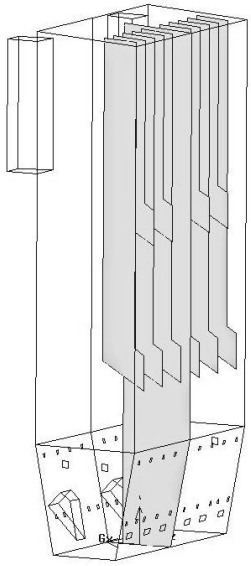

Figure 1. Boiler geometry

MEASUREMENTS AND SIMULATION SETUP
The combustion chamber geometry of the Ruzhou power plant is shown in Figure 1 in the simplified form in which it is described in the CFD simulation. The conical bottom section of the furnace is refractory lined while other walls are membrane walls. The figure also shows the six hanging super heaters and four re-heaters in the upper part of the furnace. In the middle of the furnace there is a membrane wall that to a large extent splits the furnace in two sections. This allows flexible

furnace operation. In the case measured and simulated in the present work, more fuel and secondary air was fed to one side of the furnace.

In the boiler, coal is fed through six coal feeders located on the front wall. Secondary air enters from two levels at the front and back walls and some air also enters from the sides of the furnace from the four ash coolers located next to the corners of the furnace. The furnace is equipped with two cyclones, of which only the exit and return channels, shown in the picture, are included in the simulated domain.

Primary and secondary air flows into the furnace and coal feed rates are listed in Table 1. The primary air flow is 41% of the total air flow, which in this geometry results in a relatively low primary fluidization velocity (1.96 m/s at assumed 800 °C temperature). The total coal feed rate is adjusted on basis of the oxygen balance based on the measured O_2 concentration in the backpass.

Table 1. Air and fuel flow rates.

Air flow	**Primary**	**To coal feeders**	**To ash coolers**	**To loop seal**		**Upper secondary**		**Lower secondary**	
				Left	**Right**	**Left**	**Right**	**Left**	**Right**
kg/s	46.5	4.7	10.7	0.34	0.35	21.7	9.2	19.1	11.0

Fuel flow	**Feeder 1**	**Feeder 2**	**Feeder 3**	**Feeder 4**	**Feeder 5**	**Feeder 6**
kg/s	6.3	7.9	8.1	7.9	4.0	3.0

The fuel used in the experiments was a local high ash coal. Its size distribution and primary fragmentation tendency were measured. The initial size distribution and the distribution after primary fragmentation, which was used as an input to the simulation, are shown in Table 2.

Table 2. Particle size distribution of coal before and after primary fragmentation.

Size, mm	**0.0 - 0.5**	**0.5 – 1.0**	**1.0 – 2.0**	**2.0 - 3.2**	**3.2 – 6.0**	**> 6.0**
Before, %	28.7	13.9	25.1	15.2	10.1	7.0
After, %	31.2	16.2	26.3	11.1	8.5	6.7

The chemical composition of the fuel is listed in Table 3. The heating value of the fuel is 7.7 MJ/kg (a.r.).

Table 3. Fuel analysis

Volatiles [wt% daf]	**Proximate [wt% a.r.]**			**Ultimate [wt% daf]**				
	Comb.	**Ash**	**Moist.**	**C**	**H**	**O**	**S**	**N**
41.7	32.6	62.6	4.8	56.9	7.7	32.1	1.8	1.6

Pressure and temperature profiles, flue gas composition and heat exchanger data were collected during the experiment from the control system. A bottom ash sample was taken for analysis of particle size distribution and the amount of unburned in each size fraction. Additional measurements were carried out at four distances from the wall through four measurement ports on the right side wall of the furnace. The first measurement location was at 17.9 m height, the second at 27.4 m height, the third in the cyclone inlet channel at 30.6 m height and the fourth at cyclone outlet. In addition to measurements of temperature and gas composition, a suction probe was used to take samples of the solids.

The measurements were conducted in between normal power plant operation so that the time the power plant was kept at the studied condition was only a few hours. Thus the bed inventory and particle size distribution differ from what would prevail at steady state.

MODELING

Hydrodynamic model for gas-solid suspensions

A steady-state CFD modeling approach based on time-averaged Eulerian-Eulerian equations for hydrodynamics of gas-solid suspensions was introduced in Taivassalo *et al.* (1). Time-averaged continuity and momentum equations were developed by averaging the corresponding time-dependent equations over time and, by ignoring density fluctuations, they can be summarized for a phase *q* as follows

$$\nabla \cdot \overline{\rho}_q \overline{\alpha}_q \mathbf{U}_q = 0 \tag{1}$$

$$\begin{aligned} \nabla \cdot \overline{\alpha}_q \overline{\rho}_q \mathbf{U}_q \mathbf{U}_q = {} & \overline{\alpha}_q \overline{\rho}_q \mathbf{g} - \overline{\alpha}_q \nabla \overline{p} - \overline{\alpha_q' \nabla p'} + \nabla \cdot \overline{\alpha_q \boldsymbol{\tau}_q} + \nabla \cdot \overline{\alpha_q \boldsymbol{\tau}^M{}_q} \\ & + (-1)^{(\delta_{qs}+1)} \overline{K_{gs}\left(\mathbf{u}_g - \mathbf{u}_s\right)} - \delta_{qs} \nabla \overline{p}_s - \nabla \cdot \overline{\rho}_q \overline{\alpha_q \mathbf{u}''_q \mathbf{u}''_q} \end{aligned} \tag{2}$$

Here ρ is the density, α volume fraction, p pressure, p_s solid pressure, $\mathbf{g}$ gravitational acceleration, K inter-phase momentum transfer coefficient, δ_{gs} Kronecker delta, $\boldsymbol{\tau}$ laminar stress, and $\boldsymbol{\tau}^M$ local-scale turbulent stress. The time average, also called the Reynolds average, of a variable φ is denoted by $\bar{\varphi}$ and the fluctuation part by $\varphi' = \varphi - \bar{\varphi}$. In the equations above, $\mathbf{u}$ is the instantaneous velocity, $\mathbf{U}_q$ is the Favre average or phase-weighted average velocity $\mathbf{U_q} = \overline{\alpha_q \mathbf{u_q}}/\overline{\alpha_q}$ and $\mathbf{u}_q'' = \mathbf{u}_q - \mathbf{U}_q$ is the velocity fluctuation. The gas phase is denoted by *g* and solid phase by *s*.

Equation (2) contains a number of terms that need to be modeled. Compared to the transient equations, the averaging process produces new terms due to correlations between fluctuations in velocities, volume fractions, pressure and local stresses. The terms on the right hand side in Equation (2) are, from left to right, the gravitation, pressure, pressure fluctuation, laminar stress, turbulent stress, drag force, solid pressure, and Reynolds stress terms. The gravitation and pressure terms can be directly calculated from the time-averaged flow properties but for the rest of the terms closure relations need to be developed. In Taivassalo *et al.* (1), closure relations were derived on the basis of transient simulation data. Taivassalo *et al.* (1) solved only the normal Reynolds stresses for the solid phase from balance equations, while in the present work also the cross terms are included in a similar manner. The other terms are modeled through algebraic correlations. In the description of mixing in the gas and solid phases, correlations for the time scales of the velocity fluctuations based on the results of Peltola & Kallio (3) are employed.

Homogenous chemistry

In the time-averaged transport equation for a gas-phase species, the velocity fluctuations (Reynolds stresses) and their time scales are used to estimate a

local value for an isotropic dispersion coefficient needed in the calculation of the dispersion flux. The gas phase is described as a mixture of seven species, O_2, N_2, CO_2, CO, H_2O, H_2 and a general volatilized gas CH_xO_y that represents the complex gas mixture released during devolatilization. In this work, the complex gas-phase chemistry is modeled by the following net reactions

R1: $CH_xO_y + (x/2+1-y)/2\ O_2 \rightarrow CO + x/2\ H_2O$

R2: $CO + 0.5O_2 \rightarrow CO_2$

R3: $H_2 + 0.5\ O_2 \rightarrow H_2O$

The time-averaged reaction rates are assumed to be limited by the gas-phase mixing approximated by an isotropic dispersion coefficient. The time-averaged mass-weighted mass fractions are used as such in the calculation of the reaction rates.

Modeling fuel particles

The Lagrangian particle tracking approach is employed in this work to represent the complex and varying behaviour of different kind of reactive particles with broad size distributions. The drag forces on the tracked particle due to interaction with both (solid and gas) phases are taken into account. The solid-phase average velocity field, velocity fluctuations and time scales are used in determining the instantaneous velocity components for the tracked particle. For the drag force between the fuel particles and the Eulerian solid phase, the model of Syamlal (4) is applied. Large fuel particles leaving the furnace that are assumed to be separated by the cyclone, are returned to the furnace with the solid bed material. Evaporation, devolatilazation, combustion and gasification of the fuel particles are modelled with the approach presented by Taivassalo et al. (2)

Heat transfer

In the simplified time-averaged energy balance equation, the magnitude and time scales of the velocity fluctuations are used to predict a representative value for the isotropic heat transfer coefficient. In the calculation of the heat exchange coefficient h_{sg}, the model of Gunn (8) is used to evaluate the Nusselt number. The heat transfer coefficient between the gas-solid suspension and the walls is evaluated utilizing the model of Nirmal Vijay and Reddy (9).

Simulation

The Ansys Fluent 14 (Ansys, 10) code was used to obtain a steady-state solution of the coupled transport equations, Eqs. (1), (2), (3) and (4) as well as the corresponding transport equation for the Reynolds stresses, and to carry out the tracking of representative fuel particles. In addition, in the current case the simplest radiation model, the P1 model, of Fluent was activated and the solids volume fraction was used to evaluate the dispersion and scattering coefficient. In typical CFB conditions, the range of visibility is so short that even the P1 model, suitable for optically thick media (Ansys, 10), is considered satisfactory. The computational mesh consisted of approximately 2 million elements.

A major weakness of the Eulerian model used in the present work is the assumption of a single, locally fixed particle size. To approximate the distribution of particles of different size in the furnace, the particle diameter was set as a function of riser height. At the bottom the size was set at 0.45 mm on basis of an

analysis of bottom ash samples and at the top at 0.117 mm, which was roughly the median size in the samples taken at 17.9 m height. Such an approach means that to local mean particle diameter has to be chosen a priori and it is not affected by changes in the flow solution. This kind of modelling approach should only be considered as a temporary approximation to allow development of the other submodels. The present simulation is particularly sensitive to this limitation, because the low primary fluidization velocity causes a steep mean diameter change above the bottom bed, as the gas velocity is too low to lift anything but the small particles.

The bed mass was estimated from the measured pressure profile. Outlet boundary pressures are set the same for both outlets, because the pressure measurement provided by the automation system for the left outlet was not credible

RESULTS AND DISCUSSION

The Lagrangian description of the fuel particles proved very time consuming in such a large boiler. The fuel particles spend considerable time in the boiler which requires a large number of time steps to be calculated for each particle. As the results affect the Eulerian flow solution, iteration between the Eulerian and Lagrangian results is required. It might be possible to reduce the computational effort by optimizing to code, but this may require a different modelling platform.

The higher air and fuel mass flows in the left half of the furnace produce asymmetric velocity and temperature fields as seen as higher flow velocities and temperature in Figure 2. Generally there is a falling wall layer of solid on all the walls and heat exchangers. The secondary air inlets tend to form high velocity vertical channels all the way to the outlets. There is significant variation in the wall layer thickness in different locations, but since no velocity profile data is available from the furnace, there is significant uncertainty in the assessment of the correctness of the results.

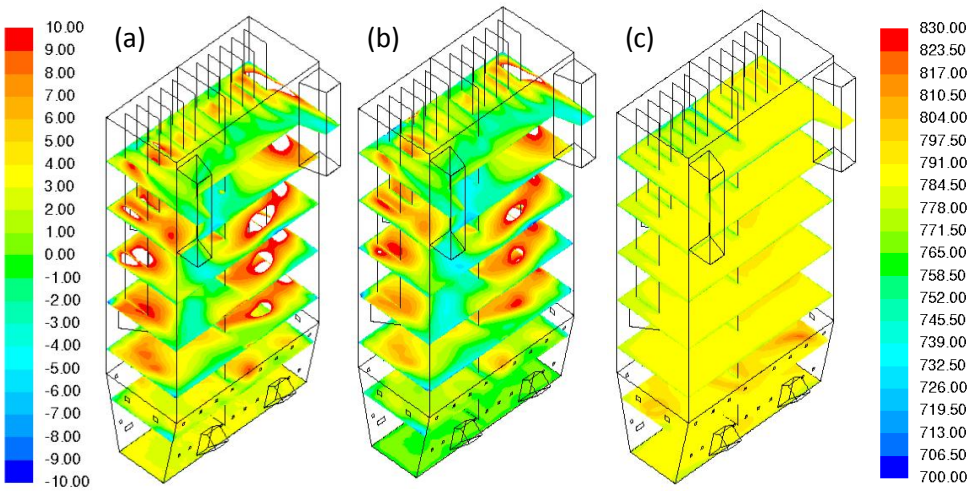

Figure 2. Contours of simulated gas (a) and solids (b) vertical velocities [m/s] and gas temperature [°C] (c).

Similar asymmetry can be seen in the volume fraction contours of Figure 3. When the vertical pressure profiles are compared to the measured ones, the measurements show much stronger asymmetry. Because credible pressure data was available only for the right outlet, it is unclear if the assumption of the same pressure at both outlets is valid. However, the overall trend of the pressure profile matches well with the measurements.

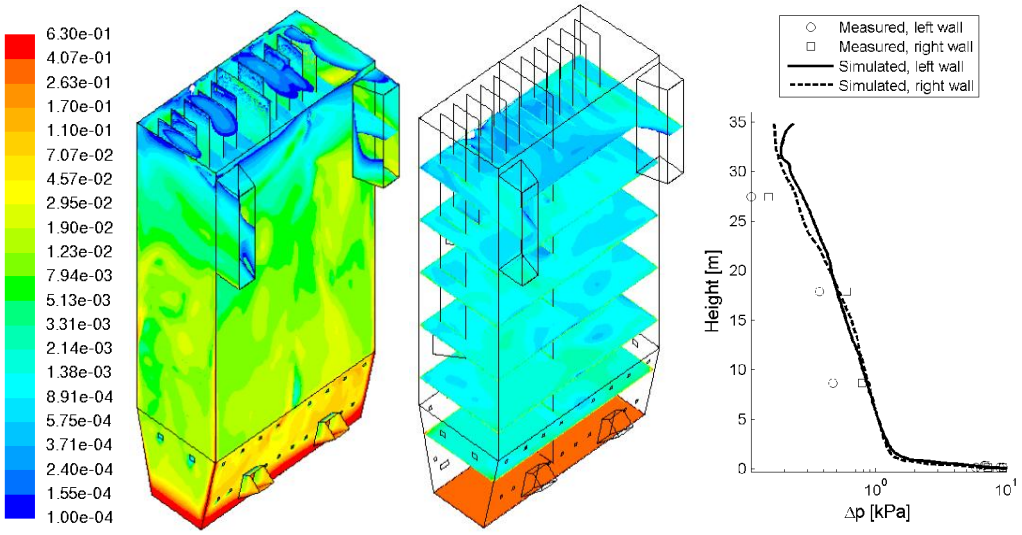

Figure 3. Solids volume fraction contour and comparison of simulated pressure profiles to measured values.

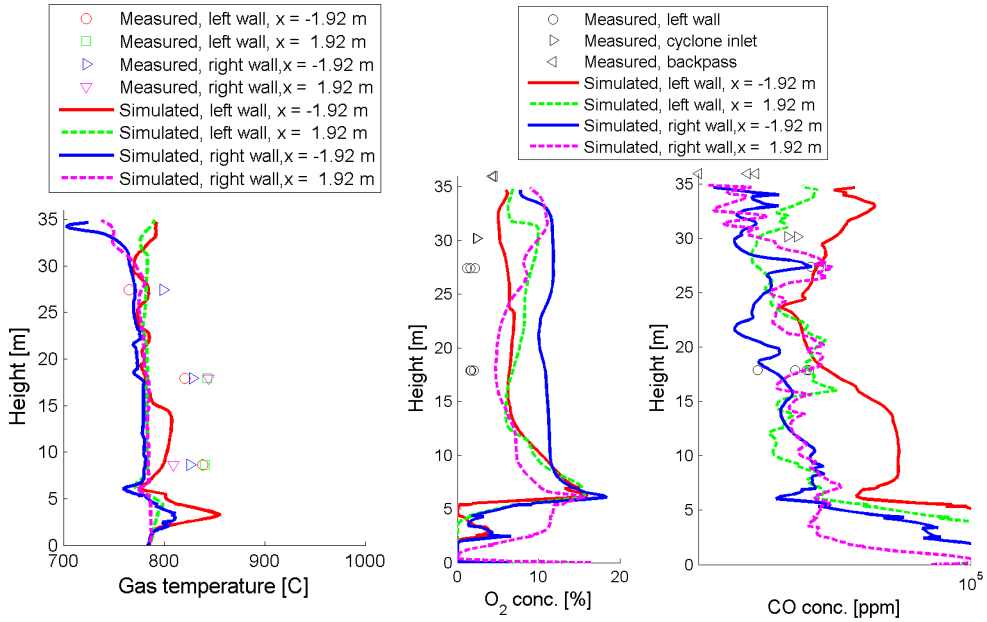

Figure 4. Comparison of simulated vertical gas temperature, O_2 and CO concentration profiles to measured values.

Figure 4 shows a comparison of measured temperatures and O_2 and CO concentrations to selected vertical profiles from the simulation. The measurement locations do not coincide exactly with the sampling lines of the simulation in all

locations. The simulated profiles are quite uneven, showing sharp local variations in the temperature and species concentrations. This may be a symptom of inadequate number of Lagrangian fuel particles. Highest temperatures have been measured at 17.9 m height, but the simulated temperatures are generally lower than measured.

The vertical oxygen concentration profiles show a region of low oxygen below the secondary air level. At the measurement location near the walls the simulated oxygen concentrations are higher than measured. This is probably an indication that the vertical channels formed by the secondary air jets in the simulations may not be as strong in the real boiler. There is a lot of variation in the vertical CO profiles, but if any conclusion can be drawn, at the measurement locations the results are in similar range.

CONCLUSIONS

A steady-state simulation approach was applied to a 135 MWe circulating fluidized bed combustor to examine its behavior in a commercial scale CFB. The results were presented and compared with measurement data from a measurement campaign carried out at the power plant. Temperature, pressure and gas composition data was compared with measurements.

While the Eulerian time-averaged simulation is quite fast, iterating the Eulerian solution and the Lagrangian simulation of the fuel particles proved very time consuming in a large boiler. There is a possibility for some improvement by optimizing the Lagrangian particle code, but it is likely that if a Lagrangian fuel description is used, the Lagrangian portion of the simulation will remain as the limiting factor for simulation speed.

The simulation results show the typical characteristics of a CFB, i.e. a dense suspension region at the furnace bottom and more dilute conditions higher up. Dense, falling layers of solids are found on the walls and heat exchangers. The asymmetric fuel and air inlets produce an asymmetric flow field also in the simulation, but the difference is not as large as in the pressure measurements. In the simulation, the pressure boundary condition was uniform at both outlets, because credible pressure measurement data was available only from the right outlet. The general trend of the pressure profiles matches well with the measurements.

Gas composition profiles show local variation, possibly due to an inadequate number of Lagrangian fuel particles. Simulated oxygen concentration at the near-wall measurement locations is higher than measured, indicating that the near-wall channeling effect of the secondary air may be over predicted in the simulation.

The observed probable discrepancies to reality can be a consequence of the fixed vertical mean particle diameter profile and of the limited amount of data used as basis for the derivation of equation closures for the time-averaged balance equations. The present simulation is particularly sensitive to the fixed particle diameter approximation, because the low primary fluidization velocity creates a very steep mean diameter gradient above the bottom bed, as the gas

velocity is too low to lift anything but the small particles. The small particle size in the upper furnace is outside the parameter range used in the closure derivation and thus the closures should in the future be extended to smaller particle sizes. Similarly, new data on flow behavior near secondary air streams is needed to improve the models. All in all, the results demonstrate a need for a better modeling of the solids size distribution and sensitivity of the closure models to changes in the operational conditions.

ACKNOWLEDGMENT

The authors gratefully acknowledge the financial support of Tekes, VTT Technical Research Centre of Finland, Etelä-Savon Energia Oy, Fortum, Metso Power Oy and Numerola Oy, and the support from Saarijärven Kaukolämpö Oy. The invaluable contribution of the powerplant personnel and the assistance of all the people participating in the experiments are gratefully acknowledged.

NOTATION

g	gravitational acceleration	α	volume fraction
K	drag coefficient	δ_{ij}	Kronecker delta
p	pressure	ρ	density
u	velocity	σ	standard deviation
x	spatial coordinate	τ	stress

REFERENCES

1. Taivassalo, V., Kallio, S., Peltola, J., On time-averaged CFD modeling of circulating fluidized beds, accepted for presentation at the 12th Int. Conf. Multi-Phase Flow in Industrial Plants, Ischia, Italy, September, 2011.
2. Taivassalo, V., Peltola, J., Kallio, S., Time-averaged CFD modeling of a circulating fluidized bed combustor, FBC21, Naples Italy, 2012.
3. Peltola, J., Kallio, S.: Estimation of turbulent diffusion coefficients in a CFB on basis of transient CFD simulations, FBC21, Naples Italy, 2012.
4. Syamlal, M.: The particle-particle drag term in a multiparticle model of fluidization. National Technical Information Service, Springfield, VA, USA. DOE/MC/21353-2373,NTIS/DE87006500 1987 (referenced in Ansys Inc., 2010).
5. Palchonok, G.: Heat and Mass Transfer to a Single Particle in Fluidized Bed, Doctoral thesis, CTH, Sweden, 1998.
6. Ross, D.P., Heidenreich, C.A., and Zhang, D.K.: Devolatilisation times of coal particles in a fluidised-bed. Fuel 79 (2000) 873-883.
7. Konttinen, J., Kallio, S., Kilpinen, P.: ”Oxidation of a single char particle – Extension of the model and re-estimation of kinetic rate constants”, Report 02-4, Åbo Akademi University, Process Chemistry Group, 2002.
8. Gunn, D.J.: Transfer of heat or mass to particles in fixed and fluidized beds, Int. J. Heat Mass Transfer, 21 (1978) 467-476 (in Ansys Inc., 2010).
9. Nirmal Vijay, G., Reddy, B.V.: Effect of dilute and dense phase operating conditions on bed-to-wall heat transfer mechanism in a circulating fluidized combustor. Int. J. Heat and Mass Transfer 48 (2005) 3276-3283.
10. Ansys inc.: Ansys FLUENT theory guide, Release 14.0, 2011.